

Investigation on the thermal properties, density and degradation of quaternary iron and titanium phosphate based glasses

SIS Shaharuddin¹, I Ahmed ², D Furniss³, AJ Parsons², CD Rudd²

¹Department of Mechanical Engineering, Kulliyah of Engineering, International Islamic University Malaysia, 53100 Gombak, Malaysia

²Faculty of Engineering, Division of Materials, Mechanics and Structures, University of Nottingham, NG7 2RD, UK

³Faculty of Engineering Division of Electrical Systems and Optics, University of Nottingham, NG7 2RD, UK

shaimihezri@iiu.edu.my

Abstract. The possibility of producing phosphate based glasses (PBG) with tailored degradation profile allows for unique utilisation in biomedical application. Various compositions in the phosphate based glass (PBG) system of $(50-x)\text{P}_2\text{O}_5-40\text{Ca}-(5+x)\text{Na}-5\text{TiO}_2$ and $(50-x)\text{P}_2\text{O}_5-40\text{Ca}-(5+x)\text{Na}-5\text{Fe}_2\text{O}_3$, where $x=5$ and 10 were prepared and characterised. Method as differential scanning calorimetry (DSC) has been used to characterise the thermal properties of these phosphate based glasses. It was observed that both glass transition temperature (T_g) and onset of crystallisation temperature (T_x) increased with increasing phosphate content. In addition, T_g values were found to be higher for the $\text{P}_2\text{O}_5\text{-CaO-Na}_2\text{O-TiO}_2$ glass system compared to $\text{P}_2\text{O}_5\text{-CaO-Na}_2\text{O-Fe}_2\text{O}_3$ glass system. The density result showed that increasing the P_2O_5 content at the expense Na_2O led to a decrease in density for both glass systems. The dissolution study of these glasses was conducted in phosphate buffered saline (PBS). It was observed that the dissolution rate of $\text{P}_2\text{O}_5\text{-CaO-Na}_2\text{O-Fe}_2\text{O}_3$ glass system was higher than the $\text{P}_2\text{O}_5\text{-CaO-Na}_2\text{O-TiO}_2$ glass system. The dissolution rate for both glass systems was in the order of $10^{-6} \text{ g cm}^{-2} \text{ hr}^{-1}$.

1. Introduction

Recently, phosphate based glasses (PBG), based on the P_2O_5 glass-forming network have been developed for use as structural reinforcement in resorbable matrices. The possibility of producing PBG in different forms, such as amorphous fibres, bulk and powders allows for a wide range of applications for these materials [1]. Recently resorbable fibre reinforced composite materials encompassing an appropriate combination of initial strength and stiffness, biocompatibility and capable for intraoperative re-shaping (where needed) are of considerable interest since subsequent absorption has two very important advantages [2, 3]:

- Absorption process reduces the device cross-section and/or the material's elastic modulus, thus load can be gradually transferred to the healing bone
- With complete absorption of the device, a second surgical removal process is not necessary



Ahmed *et al.* [4] had successfully drawn fibres via the melt drawn method for glasses in the system of $50\text{P}_2\text{O}_5-(x+5)\text{CaO}-(x-5)\text{Na}_2\text{O}$ however, biocompatibility studies for the fibres revealed that these compositions were too soluble for cell attachment and proliferation [5, 4]. In contrast, biocompatibility studies in which either Fe_2O_3 or TiO_2 was introduced in the PBG composition in relatively low amounts into ternary $\text{P}_2\text{O}_5\text{-CaO-Na}_2\text{O}$ has shown success in obtaining sufficient cellular attachment and proliferation [6-8]. Therefore complex glass systems have been developed and investigated such as $\text{P}_2\text{O}_5\text{-CaO-Na}_2\text{O-Fe}_2\text{O}_3$ [7, 9], $\text{P}_2\text{O}_5\text{-CaO-Na}_2\text{O-TiO}_2$ [10, 6, 11, 8] and $\text{P}_2\text{O}_5\text{-CaO-Na}_2\text{O-MgO}$ [12-14]. Indeed, addition of these higher valence components showed significant improvement in their thermal properties and chemical durability due to the formation of relatively stable M-O-P [15] bonds (where M is the modifying oxides).

This study was undertaken to compare the effect of Fe and Ti additions in the system of $(50-x)\text{P}_2\text{O}_5\text{-}40\text{Ca}\text{-(}5+x\text{)Na-}5\text{TiO}_2$ and $(50-x)\text{P}_2\text{O}_5\text{-}40\text{Ca}\text{-(}5+x\text{)Na-}5\text{Fe}_2\text{O}_3$, where $x=5$ and 10 for their thermal, density and dissolution properties. These glass systems were also interchangeably referred to as $\text{P}_2\text{O}_5\text{-CaO-Na}_2\text{O-TiO}_2$ and $\text{P}_2\text{O}_5\text{-CaO-Na}_2\text{O-Fe}_2\text{O}_3$.

2. Materials and Methodology

2.1. Glass preparation

Four different glass compositions were prepared using sodium dihydrogen phosphate (NaH_2PO_4 , Sigma Aldrich, UK, $\geq 99\%$), calcium hydrogen phosphate (CaHPO_4 , Sigma Aldrich, UK, $98\text{-}105\%$), phosphorous pentoxide (P_2O_5 , Sigma Aldrich, UK, $>98\%$), iron (III)-phosphate dehydrate ($\text{FePO}_4\cdot 2\text{H}_2\text{O}$, Sigma Aldrich, UK, $\geq 26\%$) and titanium (IV) oxide (TiO_2 , Riedel-de Haen, Germany, $\geq 99.5\%$) (See table 1 for glass batch composition in mol% and glass code). The precursors were weighed and transferred to a 100 ml volume Pt/5% Au crucible (Birmingham Metal Company, U.K.).

Table 1. Glass nominal batch compositions in mol% and respective glass codes for $\text{P}_2\text{O}_5\text{-CaO-Na}_2\text{O-TiO}_2$ and $\text{P}_2\text{O}_5\text{-CaO-Na}_2\text{O-Fe}_2\text{O}_3$ glass systems and glass production temperature. (Note: The glass batch composition, e.g. P45 Ca40 Na10 Fe5 denotes 45 mol% P_2O_5 -40 mol% CaO -10 mol% Na_2O -5 mol% Fe_2O_3).

Glass batch composition /Glass code	P_2O_5 / mol%	CaO / mol%	Na_2O / mol%	Fe_2O_3 / mol%	TiO_2 / mol%	Dry/melt temperature / °C	Casting temperature / °C
P45 Ca40 Na10 Fe5	45	40	10	5	-	400/1100	460
P50 Ca40 Na5 Fe5	50	40	5	5	-	400/1100	480
P45 Ca40 Na10 Ti5	45	40	10	-	5	400/1300	470
P50 Ca40 Na5 Ti5	50	40	5	-	5	400/1300	490

The samples were dehydrated for 30 min followed by melting in a furnace at the corresponding temperatures for 90 min as given in table 1. They were then poured onto a steel plate and left to cool to room temperature. Once cool, the as-quenched glasses were crushed into powders and sieved to obtain glass particles with a diameter in the range of 106 and 53 microns, which were used for differential scanning calorimetry, via DSC (SDT Q600, UK) to determine the glass characteristic temperatures. For the glass dissolution study, glasses were cast into a cylindrical graphite moulds with an inner diameter of 9 mm and an outer diameter of 19 mm. Upon cooling these glasses were annealed using the same regime mentioned above. The glass rods were cut accordingly into thickness of 5 mm using a diamond

edge circular saw and were polished with 1000 grit SiC paper and then cleaned by immersing in an acetone (Sigma Aldrich, UK, $\geq 99.5\%$).

2.2. SEM/EDX analysis

Small pieces of the quenched glasses were cast into epoxy resin and then polished with SiC paper and diamond cloths using oil as the lubricating medium. The samples were then cleaned using industrial methylated spirit (IMS, Sigma Aldrich, UK, $\geq 99.5\%$) and dried before being carbon coated. These samples then underwent secondary electron microscopy/energy dispersive X-ray analysis (SEM/EDX). SEM/EDX was conducted using an Oxford Instruments INCA EDX system with a Si-Li crystal detector. The EDX was attached to a scanning electron microscope (Philips XL 30 SEM, UK) with a tungsten filament electron source, which was operated in backscattered electron mode. Analysis was conducted on 5 separate spots on each glass sample.

2.3. Differential scanning calorimetry

In order to obtain a complete glass characteristic property up to the glass liquidus temperature, a high temperature differential scanning calorimetry, DSC instrument was used (TA Instruments SDT Q600, UK). The samples were subjected to programmed heating cycle to introduce a known thermal history. In the first programmed cycle, fresh samples ($n=2$) of approximately 30 mg samples of the glass powders (diameter in the range of 106 and 53 microns) were heated from room temperature to $T_g + 20^\circ\text{C}$ at $20^\circ\text{C min}^{-1}$, held isothermally for 15 minutes then cooled at $10^\circ\text{C min}^{-1}$ to room temperature to give a known thermal history. In the second programmed cycle, the samples were heated from room temperature to 1100°C at $20^\circ\text{C min}^{-1}$ under a flowing argon gas.

2.4. Density

The density of the glasses was determined using a Micromeritics AccuPyc 1330 helium pycnometer (Norcross, GA, USA). The volume of the sample is determined by measuring the difference in helium pressure before and after loading. Triplicate bulk glass samples with an average weight of approximately 6.5 g were performed for the density measurements.

2.5. Dissolution study

Phosphate buffered saline (PBS) was prepared by dissolving PBS tablets (Sigma Aldrich, UK) in deionised water in the ratio of 1 tablet : 200 ml. Three PBG discs with diameter and thickness of approximately 9 mm and 5 mm respectively were immersed in 30 ml PBS in glass vials. These samples were then placed into an oven at 37°C . The surface area of the glass disks was calculated from the dimensions obtained via a pair of electronic digital callipers (Mitutoyo, Japan). At various time points, the disks were taken out of their respective glass vials, and excess moisture was removed by blotting the samples dry with tissue. The mass of the glass discs was measured using a digital balance (Sartorius, UK) up to 4 decimal points. During the first week, the mass loss and surface area were measured at day 1, 2, 3 and 6. The following weeks during the first month, measurements mentioned above were conducted at 2 time points per week. Since no rapid change in terms of mass was observed, the time point during the second and third month was reduced to once per week. The dissolution media was replaced with fresh solution of PBS at time point 1, 2, 3 and 6 during the first week and at two points per week for the rest of the study. In order to obtain the rate of mass loss, data obtained were plotted in terms of mass loss per unit area.

3. Results

3.1. SEM/EDX analysis

Table 2 shows the elemental compositions of the glasses investigated. Both Na₂O and Fe₂O₃ content measured by SEM/EDX were found to be close to actual values expected. However, the amount of phosphate (P₂O₅) was only slightly higher than expected.

Table 2. SEM/EDX analysis of glasses produced in the P₂O₅-CaO-Na₂O-Fe₂O₃ and P₂O₅-CaO-Na₂O-TiO₂ glass system.

Glass code	Na ₂ O / mol%	P ₂ O ₅ / mol%	CaO / mol%	Fe ₂ O ₃ / TiO ₂ / mol%
P45 Ca40 Na10 Fe5	10.2±0.1	47.3±0.1	38.1±0.1	4.3±0.1
P50 Ca40 Na5 Fe5	5.5±0.1	52.0±0.1	38.0±0.2	4.4±0.1
P45 Ca40 Na10 Ti5	9.1±0.1	48.1±0.1	38.0±0.2	4.7±0.1
P50 Ca40 Na5 Ti5	4.7±0.1	52.6±0.2	38.1±0.2	4.7±0.2

3.2. Glass thermal characteristic analysis (T_g , T_x , T_c , T_m , T_L)

It was observed that higher T_g (glass transition temperature) and T_x (onset of crystallisation temperature) values were obtained with increasing phosphate content in the P₂O₅-CaO-Na₂O-Fe₂O₃ glass system (see table 3). In this glass system, the T_g for P45 Ca40 Na10 Fe5 and P50 Ca40 Na5 Fe5 is 469°C and 488°C respectively. Both thermal scans of P45 Ca40 Na10 Fe5 and P50 Ca40 Na5 Fe5 were characterised by the presence of 3 crystallisation peaks. The crystalline peaks (T_c) detected for P45 Ca40 Na10 Fe5 were sharper and occurred at 586°C, 650°C and 734°C. The first crystallisation peak for P50 Ca40 Na5 Fe5 occurred at 609°C followed by a broad crystallisation peak with 2 distinct smaller peaks. Single melting peak (T_m) was found for P45 Ca40 Fe5 at 883°C whilst two melting peaks were detected for P50 Ca40 Fe5 at 828°C and 906°C. It was also observed that the liquidus temperature (T_L) increased with increasing phosphate content.

Table 3. The thermal characteristics (T_g , T_x , T_c , T_m , T_L) for (50-x)P₂O₅-40CaO-(5+x)Na₂O-5Fe₂O₃ and (50-x)P₂O₅-40CaO-(5+x)Na₂O-5TiO₂ glass systems.

Glass code	T_g / °C	T_x / °C	T_c / °C	T_m / °C	T_L / °C
P45 Ca40 Na10 Fe5	469.4 ±0.5	554.1 ±0.4 469.4 ±0.5	585.6 ±1.8 650.4 ±0.6 733.6 ±0.0	883.8 ±1.5	908.8 ±0.3
P50 Ca40 Na5 Fe5	487.9 ±0.5	572.7 ±0.8	608.5 ±0.6 710.5 ±0.6 743.8 ±0.4	827.8 ±0.8 905.5 ±1.0	918.2 ±1.5
P45 Ca40 Na10 Ti5	477.2 ±0.8	570.3 ±2.7	616.4 ±3.0 699.4 ±3.4 766.6 ±0.5	969.4 ±3.3	1012.6 ±0.8
P50 Ca40 Na5 Ti5	501.9 ±0.4	616.9 ±0.3	658.6 ±2.0 790.0 ±0.3	915.6 ±1.5	932.0 ±1.1

Thermal scan of the glasses studied in the P_2O_5 -CaO- Na_2O - TiO_2 glass system showed that higher T_g and T_x values were obtained with increasing phosphate content in the P_2O_5 -CaO- Na_2O - TiO_2 glass system. In this glass system, the T_g for P45 Ca40 Na10 Ti5 and P50 Ca40 Na5 Ti5 is 477°C and 502°C respectively. The thermal scan of P45 Ca40 Na10 Ti5 revealed 3 crystallisation peaks which occurred at 616°C, 699°C and 767°C. The thermal scan of P50 Ca40 Na5 Ti5 revealed a very weak 1st crystallisation peak which occurred at 659°C and a broad peak at 790°C. With increasing phosphate content, both glasses exhibited single melting peak at 969°C and 916°C respectively. The liquidus temperature for P50 Ca40 Na5 Ti5 is slightly lower than P45 Ca40 Na10 Ti5 at 932°C and 1013°C respectively.

3.3. Density analysis

The effect of composition on the density for the P_2O_5 -CaO- Na_2O - Fe_2O_3 and P_2O_5 -CaO- Na_2O - TiO_2 glass systems is shown in figure 1 respectively. Increasing phosphate content at the expense of Na_2O led to a decrease in density from $2.8 \times 10^3 \text{ kg m}^{-3}$ to $2.7 \times 10^3 \text{ kg m}^{-3}$ in the P_2O_5 -CaO- Na_2O - Fe_2O_3 glass system. The change in density was only slightly lower in the P_2O_5 -CaO- Na_2O - TiO_2 glass systems from $2.7 \times 10^3 \text{ kg m}^{-3}$ to $2.6 \times 10^3 \text{ kg m}^{-3}$.

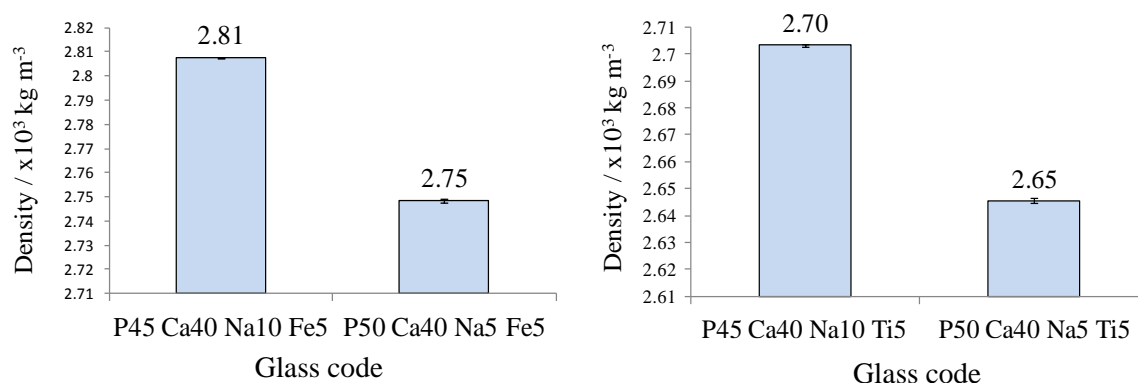


Figure 1. Effect of increasing P_2O_5 content at the expense of Na_2O on density.

3.4. Dissolution study

The mass loss per unit area was plotted against dissolution time in Figure 22 and figure 3 to yield a linear fit and the correlation coefficient, R . It was evident from both figures that the dissolution rate was almost constant throughout the immersion period. For glasses with fixed P_2O_5 content at 45 mol%, it was found that the dissolution rate obtained for Fe containing glasses was slightly higher than the Ti containing PBG. The dissolution rate per unit area obtained for P45 Ca40 Na10 Fe5 and P45 Ca40 Na10 Ti5 were $5.25 \times 10^{-6} \text{ g cm}^{-2} \text{ hr}^{-1}$ and $3.06 \times 10^{-6} \text{ g cm}^{-2} \text{ hr}^{-1}$ respectively (see figure 2). Dissolution rate per unit area obtained for PBG with fixed P_2O_5 content at 50 mol%, where the dissolution rate for P50 Ca40 Na5 Fe5 and P50 Ca40 Na5 Ti5 were $4.17 \times 10^{-6} \text{ g cm}^{-2} \text{ hr}^{-1}$ and $2.25 \times 10^{-6} \text{ g cm}^{-2} \text{ hr}^{-1}$ respectively (see Figure 3). It should be noted that the linear regression line was fitted to plots of non-linear data, and thus the dissolution rates obtained were approximation values. The dissolution rate for both PBG glass systems were in the order of $10^{-6} \text{ g cm}^{-2} \text{ hr}^{-1}$.

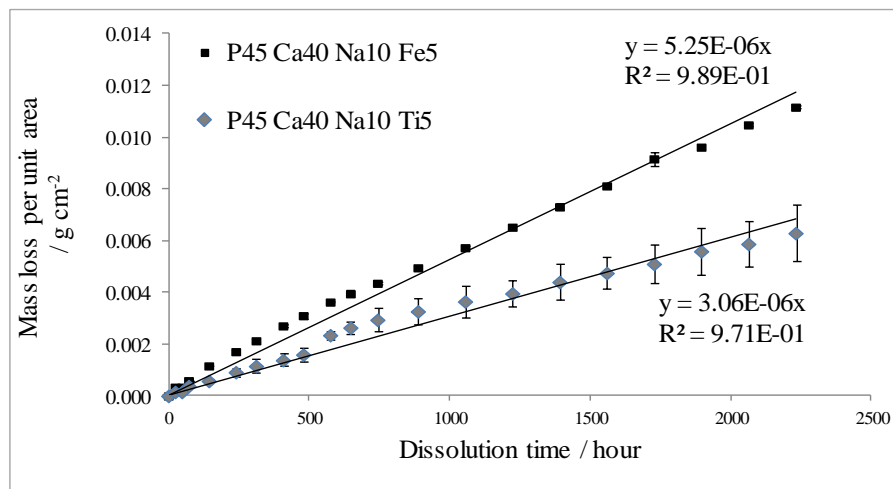


Figure 2. Comparison of mass loss per unit area versus dissolution time for glasses fixed at 45 mol% of P_2O_5 (P45 Ca40 Na10 Fe5 and P45 Ca40 Na10 Ti5) in PBS at 37°C.

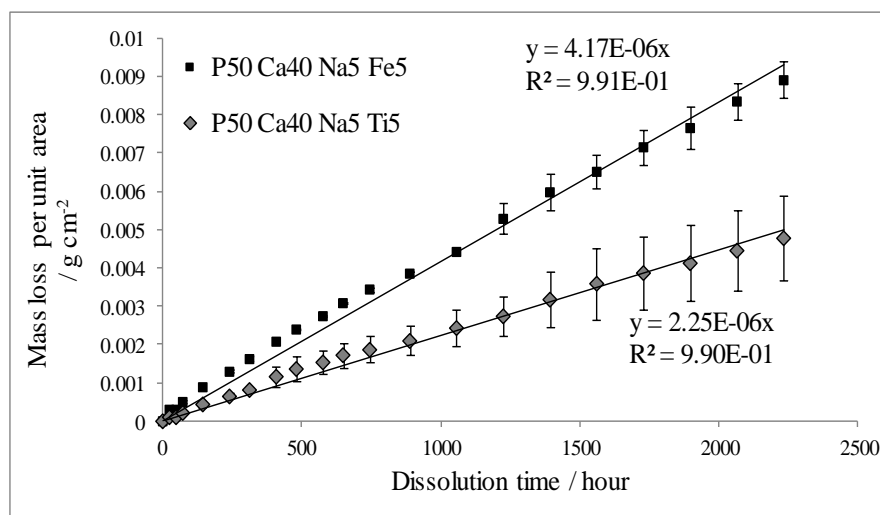


Figure 3. Comparison of mass loss per unit area versus dissolution time for glasses fixed at 50 mol% of P_2O_5 (P50 Ca40 Na5 Fe5 and P50 Ca40 Na5 Ti5) in PBS at 37°C.

It was also observed that P50 Ca40 Na5 Fe5 produced a thicker layer of white precipitation after one week of being degraded in PBS in comparison to P50 Ca40 Na5 Ti5. The precipitations were deposited unevenly on the glass surfaces for both P50 Ca40 Na5 Fe5 and P50 Ca40 Na5 Ti5 and upon drying for SEM images, as shown in figure 4 they cracked and peeled. SEM observations depicted in figure 4 showed a marked difference in the glass surface before and after the dissolution period of 90 days. The initial surface was uneven with light scratches which probably occurred as a result of the cutting and polishing process. After 90 days of immersion in PBS, the glass surface formed grooves and furrows due to corrosion. At magnification of 1500x, it can clearly be seen that the surface of the glasses P50 Ca40 Na5 Fe5 and P50 Ca40 Na5 Ti5 were covered with white deposits. In comparison, the deposits were thicker for P50 Ca40 Na5 Fe5.

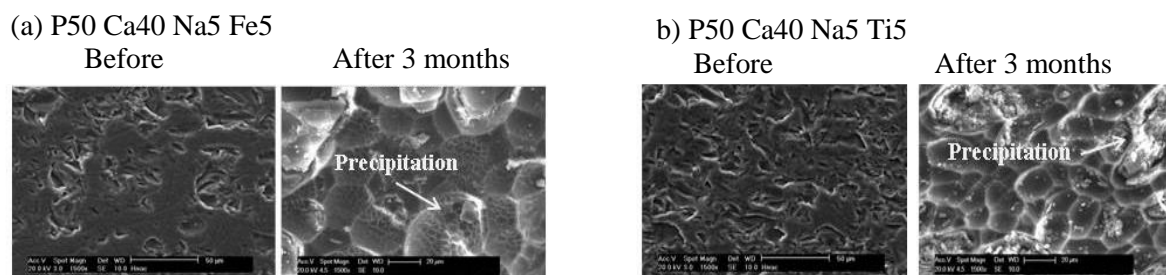


Figure 4. SEM images of the surface morphology of (a) P50 Ca40 Na5 Fe5 and (b) P50 Ca40 Na5 Ti5 glass systems before and after the dissolution period of 3 months.

4. Discussion

Phosphate based glasses can be classified into three groups which corresponds to their structure. Ultraphosphate glasses consist of three-dimensional networks of PO_4 tetrahedra which are connected via bridging oxygen atoms at three corners of most tetrahedral and glasses with more than 50 mol% P_2O_5 form this type of phosphate network. Polyphosphate glasses refer to 50 mol% P_2O_5 or less and are structurally formed by phosphate rings or chains of different chain lengths. It is accepted that the structure of ultraphosphates, metaphosphates, and polyphosphates are dominated by Q^3 and Q^2 , Q^2 , and Q^2 and Q^1 units, respectively [16]. Previous study via ^{31}P NMR analysis has shown that local structure of the glasses changes with increasing network former in which the phosphate connectivity increases as Q^1 units transform to Q^2 [5, 17]. Therefore theoretically Q^2 structure would be more dominant for phosphate glasses fixed at 50 mol% than those fixed at 45 mol%.

The glass compositions determined by SEM/EDX analysis in table 2 revealed only slight discrepancy between the nominal values and analysed SEM/EDX values for each element in the PBG system. The T_g and T_x measured via DSC increased with increasing phosphate content in both P_2O_5 -CaO- Na_2O - TiO_2 and P_2O_5 -CaO- Na_2O - Fe_2O_3 glass systems. The observed increase in T_g for the glasses studied was in good agreement with an increase in polymerisation in the glass structure with increasing Q^2 units [5] and the T_g of P50 Ca40 Na5 Fe5 was also comparable [7]. Eisenberg *et al.* [18] suggested that increase in T_g closely tracked the increasing field strength of the interstitial cations. Therefore the higher T_g values observed for Ti containing PBG system confirmed the field strength effect since TiO_2 had higher cationic field strength. Beyond the onset of crystallisation temperature, the thermal scan for P45 Ca40 Na10 Fe5 and P45 Ca40 Na10 Ti5 exhibited a 2nd sharp crystallisation peak which was linked to higher sodium content. According to Day *et al.* the addition of alkali and alkaline earth oxides leads to sharper crystallisation peaks and indicates less resistance to crystallisation when heat treated at the appropriate temperatures [19]. In general, the presence of several crystalline peaks in these glass compositions was linked to the presence of different crystal phases [20]. Both P50 Ca40 Na5 Fe5 and P50 Ca40 Na5 Ti5 had a broader crystallisation peak in the thermal scans, which was suggested to be due to either the crystalline phases consisting of very similar crystallisation peak temperatures or that the other phase(s) were present in very small quantities [7].

The density of the glasses obtained decreased with increasing phosphate content (see figure 1). Theoretically, the replacement of lighter Na_2O (molecular mass of 62 g mol⁻¹) with heavier P_2O_5 (molecular mass = 142 g mol⁻¹) should have resulted with an increase in density as found in several studies [21-23]. Ahmed *et al.* and Amos *et al.* however suggested that the density of phosphate glasses is also affected by the phosphate chain length and whether the branching group ($\text{PO}_{5/2}$, Q_3) was present in the glass structure [24, 25]. The addition of alkali and alkaline earths converts bridging oxygen to non-bridging oxygen [26] and vice versa. Therefore increase in P_2O_5 content at the expense of Na_2O converts non-bridging oxygen into bridging oxygen and it was proposed that the presence of these longer phosphate chain lengths were responsible for the lower density of the glasses [27-29].

Theoretically, it was suggested that invert PBGs, which are dominant in Q^0 and Q^1 structures [30] have better resistance against solubility [12, 31, 32, 14] since glasses with Q^2 structure were said to be more susceptible to hydrolysis [14]. It was observed that glass compositions fixed at 50 mol% of P_2O_5 especially P50 Ca40 Na5 Fe5 produced thick white deposits on the glass surface from day 7 of the dissolution study (see figure 4). SEM/EDX analysis performed on the degraded glass surface of P50 Ca40 Na5 Fe5 and P50 Ca40 Na5 Ti5 showed that the deposits also contained traces of chlorine and potassium. This was expected as the PBS tablets (Sigma Aldrich, UK) once dissolved in deionised water contained sodium chloride (NaCl), potassium chloride (KCl) and phosphate buffer solution. The formation of deposits suggested that both P50 Ca40 Na5 Fe5 and P50 Ca40 Na5 Ti5 may have degraded faster and the PBS medium became saturated at a faster rate.

According to Gao *et al.* [33] and Bourcier [34] the formation of a protective film over the hydrated layer may prevent water molecules from further diffusing into the bulk glass samples. The formation of this protective layer has also been observed by Abou Neel *et al.* in dissolution study of Fe_2O_3 containing phosphate glass fibre [35]. The ratio of oxidation states of Fe and Ti ions have not been confirmed in this study. However it is acknowledged that different oxidation state of these elements may influence the dissolution mechanism. For instance, iron is relatively insoluble in metallic form and in its +3 oxidation state, but soluble in its +2 oxidation state.

It is known that the density of the glass composition also contributes to the dissolution process [36, 37]. Sammler *et al.* [37] found that durable glass has higher density in comparison to less durable glass composition in a zinc alkali metaphosphate glass system. Both phosphate glasses of P50 Ca40 Na5 Fe5 and P50 Ca40 Na5 Ti5 had lower density and thus would have provided better ease of water diffusion into the glass to initiate the hydration process. The dissolution rate for both glass systems was in the order of $10^{-6} \text{ g cm}^{-2} \text{ hr}^{-1}$. In comparison between the two glass systems, P_2O_5 -CaO- Na_2O - TiO_2 glass system had a lower dissolution rate and was associated with the formation of a strong cross-linked structure that resisted degradation as supported from the T_g and density studies of these glasses.

References

- [1] Vitale-Brovarone C, Novajra G, Milanese D, Lousteau J and Knowles JC 2011 Novel phosphate glasses with different amounts of TiO_2 for biomedical applications: dissolution tests and proof of concept of fibre drawing. *Mat Sci and Eng C* 31 434
- [2] Andriano KP and Daniels AU 1995 Development of Phosphate-Microfiber-Reinforced Poly (orthoester) for Absorbable Orthopaedic Fixation Devices *Encyclopaedic Handbook of Biomaterials and Bioengineering: Part B* ed Wise DL (New York: M Dekker) p 333-57
- [3] Navarro M, Ginebra M, Clément J, Salvador M, Gloria A and Planell JA 2003 Physicochemical degradation of titania-stabilized soluble phosphate glasses for medical applications *J Am Ceram Soc* 86 1345
- [4] Ahmed I, Lewis M, Olsen I and Knowles JC. 2004 Phosphate glasses for tissue engineering: Part 2. Processing and characterisation of a ternary based P_2O_5 -CaO- Na_2O glass-fibre system *Biomaterials* 25 501
- [5] Ahmed I, Lewis M, Olsen I and Knowles JC. 2004 Phosphate glasses for tissue engineering: Part 1. Processing and characterisation of a ternary based P_2O_5 -CaO- Na_2O glass system. *Biomaterials* 25 491
- [6] Abou Neel EA and Knowles JC 2008 Physical and biocompatibility studies of novel titanium dioxide doped phosphate-based glasses for bone tissue engineering applications *J Mat Sci* 19 377
- [7] Ahmed I, Collins CA, Lewis MP, Olsen I and Knowles JC 2003 Processing, characterisation and biocompatibility of iron-phosphate glass fibres for tissue engineering *Biomaterials* 25 3223
- [8] Navarro M, Ginebra M and Planell JA 2003 Cellular response to calcium phosphate glasses with controlled solubility *J Biomed Mater Res A* 67A 1009

- [9] Lin ST, Krebs SL, Kadiyala S, Leong KW, LaCourse WC and Kumar B 1994 Development of bioabsorbable glass fibres *Biomaterials* 15 1057
- [10] Abou Neel EA, Chrzanowski W and Knowles JC 2008 Effect of increasing titanium dioxide content on bulk and surface properties of phosphate-based glasses *Acta Biomaterialia* 4 523
- [11] Abou Neel EA, Mizoguchi T, Ito M, Bitar M, Salih V and Knowles JC 2007 In vitro bioactivity and gene expression by cells cultured on titanium dioxide doped phosphate-based glasses *Biomaterials* 28 2967
- [12] Ahmed I, Parsons A, Jones A, Walker G, Scotchford C and Rudd C. 2010 Cytocompatibility and effect of increasing MgO content in a range of quaternary invert phosphate-based glasses *J Biomater Appl* 24 555
- [13] Samickannian A, Venkatachalam R, Nallaiyan R and Abubakkar NB 2011 Structural and textural modifications of ternary phosphate glasses by thermal treatment *Int J Appl Glass Sci* 2 222
- [14] Walter G, Vogel J, Hoppe U and Hartmann P 2001 The structure of CaO-Na₂O-MgO-P₂O₅ invert glass *J Non-Cryst Solids* 296 212
- [15] Minami T and Mackenzie JD 1977 Thermal expansion and chemical durability of phosphate glasses *J Am Ceram Soc* 60 232
- [16] Karabulut M, Metwalli E, Wittenauer AK, Brow RK, Marasinghe GK, Booth CH, Bucher JJ and Shuh DK 2005 An EXAFS investigation of rare-earth local environment in ultraphosphate *J Non-Cryst Solids* 351 795
- [17] Kiani A, Cahill LS, Abou Neel EA, Hannab JV, Smith ME and Knowles JC 2010 Physical properties and MAS-NMR studies of titanium phosphate-based glasses *Mater Chem Phys* 120 68
- [18] Eisenberg A, Farb H and Cool LG 1966 Glass transitions in ionic polymers *J Polym Sci A* 4 855
- [19] Day DE, Ray CS, Marasinghe K, Karabulut M and Fang X 2000 An alternative host matrix based on iron phosphate glasses for the vitrification of specialized waste form (Rolla: Graduate Center for Materials Research, University of Missouri-Rolla) p 1-39
- [20] Moesgaard M and Yue Y 2009 Compositional dependence of fragility and glass forming ability of calcium aluminosilicate melts *J Non-Cryst Solids* 355 867
- [21] Li Y, Yang J, Xu S, Wang G and Hu L 2005 Physical and thermal properties of P₂O₅-Al₂O₃-BaO-La₂O₃ glasses *J Mater Sci Technol* 21 391
- [22] Mošner P, Vosejpková K, Koudelka L, Montagne L and Revel B 2010 Structure and properties of ZnO-B₂O₃-P₂O₅-TeO₂ glasses *Mater Chem Phys* 124 732
- [23] Wilder JA and Shelby JE 1984 Property variation in alkali alkaline-earth metaphosphate glasses *J Am Ceram Soc* 67 438
- [24] Ahmed AA, Ali AA, Mahmoud DA and El-Fiqi AM 2011 Preparation and characterization of antibacterial P₂O₅-CaO-Na₂O-Ag₂O glasses *J Biomed Mater Res A* 98 132-42
- [25] Amos RT and Henderson GS 2003 The effects of alkali cation mass and radii on the density of alkali germanate and alkali germano-phosphate glasses *J Non-Cryst Solids* 331 108
- [26] Harper CA 2001 Handbook of ceramics, glasses and diamonds (United States of America: McGraw Hill)
- [27] Garbarczyk JE, Wasiucionek M, Jóźwiak P, Tykarski L and Nowiński JL 2002 Studies of Li₂O-V₂O₅-P₂O₅ glasses by DSC, EPR and impedance spectroscopy *Solid State Ionics* 154-155 367
- [28] Shih PY 2001 Preparation of lead-free phosphate glasses with low T_g and excellent chemical durability *J Mater Sci Lett* 20 1811
- [29] Yang R, Yinghui W, Chen Y, Hao X, Zhan J and Liu S 2010 Glass formation region of the lithium iron phosphate ternary system and the properties of obtained glasses *Ceramics* 54 352
- [30] Brow RK 2000 Review: The structure of simple phosphate glasses *J Non-Cryst Solids* 263-264 1
- [31] Brauer DS, Karpukhina N, Law RV and Hill RG 2010 Effect of TiO₂ addition on structure, solubility and crystallisation of phosphate invert glasses for biomedical applications *J Non-*

Cryst Solids 356 2626

- [32] Cozien-Cazuc S, Parsons AJ, Walker GS, Jones IA and Rudd CD 2008 Effects of aqueous aging on the mechanical properties of P40Na20Ca16Mg24 phosphate glass fibres *J Mat Sci* 43 4834
- [33] Gao H, Tan T and Wang D 2004 Dissolution mechanism and release kinetics of phosphate controlled release glasses in aqueous medium *J Control Release* 96 29
- [34] Bourcier WL 1994 Critical review of glass performance modelling (Illinois: Lawrence Livermore National Laboratory) p 1-68
- [35] Abou Neel EA, Young AM, Nazhat SN and Knowles JC 2007 A facile synthesis route to prepare microtubes from phosphate glass fibres *Adv Mater* 19 2856
- [36] Brazhkin VV, Akola J, Katayama Y, Kohara S, Kondrin MV, Lyapin AG, Lyapin SG, Tricot G and Yagafarov OF 2011 Densified low-hygroscopic form of P₂O₅ glass *J Mater Chem* 21 10442
- [37] Sammler RL, Otaigbe JU, Lapham ML, Bradley NL, Monahan BC and Quinn CJ 1996 Melt rheology of zinc alkali phosphate glasses *J Rheol* 40 285